Royal Netherlands
Meteorological Institute
Ministry of Infrastructure and the Environment

Drag at high wind velocities - a review

A. Sterl

De Bilt, 2017 | Technical report; TR-361

Drag at high wind velocities - a review

Andreas Sterl

Koninklijk Nederlands Meteorologisch Instituut (KNMI)
P.O. Box 201, NL-3730 AE De Bilt, Netherlands
phone: +31-30-2206766; e-mail: sterl@knmi.nl

July 27, 2017

Final Version

Project: Maatwerk tbv kennisontwikkeling WBI2023 en NKWK - WP3
Opdrachtgever: RWS-VWL
Interne review: Hans de Vries

Abstract

In many applications the drag coefficient is assumed to grow linearly with wind speed. This relation is based on experiments that have been conducted in the second half of the 20^{th} century. Post-2000 experiments, however, show that the drag coefficient has a maximum somewhere in the range 30-35 m/s. This report reviews the relevant literature and comes with recommendations on what parameterization of the drag coefficient should be used.

Contents

Samenvatting

De windschuifspanning τ die door de wind op het oceaanoppervlak uitgeoefend wordt, wordt gewoonlijk geparameteriseerd als

$$\tau = \rho_a \, C_D \, U_{10}^2.$$

Daarbij is ρ_a het soortelijke gewicht van lucht en U_{10} de windsnelheid op 10 m hoogte boven het zeeoppervlak. De dragcoëfficient C_D hangt af van de ruwheid van het zeeoppervlak. Omdat het zeeoppervlak met toenemende wind ruwer wordt (hogere golven), neemt de dragcoëfficient toe met toenemende wind. Meestal wordt een lineaire groei verondersteld. Er zijn echter aanwijzingen dat de dragcoëfficient boven $U_{10} \gtrsim 30$ m/s niet verder toeneemt, en bij nog hogere windsnelheden zelfs weer daalt.

In dit rapport wordt de wetenschappelijke literatuur over drag bij hoge windsnelheden gereviewd. De review is onderverdeeld in studies gebaseerd op waarnemingen, studies die proberen om de gevonden resultaten theoretisch te verklaren, en studies die het gevonden gedrag van de drag coëfficient in numerieke wind-, golf- of wateropzetmodellen toepassen.

De beschikbare studies die op in situ waarnemingen gebaseerd zijn, gebruiken uiteenlopende methodes en meettechnieken om de dragcoëfficient te bepalen. Echter, ze vinden allemaal dat de dragcoëfficient voor windsnelheden $\gtrsim 30$ m/s niet verder groeit en voor windsnelheden $\gtrsim 40$ m/s zelfs weer afneemt. De maximale C_D-waarde is $\approx (2.5 \pm 0.2) \cdot 10^{-3}$. The resultaten uit in situ metingen worden door satelliet-gebaseerde metingen met scatterometers gesteund.

Het belangrijkste resultaat van de op waarnemingen gebaseerde studies, namelijk dat de dragcoëfficient voor windsnelheden boven de 30 m/s niet verder toeneemt, kan door theoretische modellen verklaard worden, die het effect van schuim op de koppeling tussen atmosfeer en oceaan meenemen. Tenslotte stemmen resultaten van numerieke wind-, golf- en wateropzetmodellen beter overeen met waarnemingen, als een parameterisatie toegepast wordt waarbij de dragcoëfficient boven de 30 m/s niet verder toeneemt.

Dat de dragcoëfficient bij hoge windsnelheden niet verder toeneemt wordt door drie onafhankelijke onderzoekslijnen gesteund. Het

- wordt bevestigd door experimenten die onder verschillende omstandigheden doorgevoerd werden en die verschillende meetprincipes gebruiken,
- kan theoretisch verklaard worden, en
- leidt bij toepassing in numerieke modellen tot betere resultaten.

Dat geeft vertrouwen in de gevonden resultaten. Het wordt daarom aanbevolen om een formulering van de dragcoëfficient te gebruiken die deze afvlakking weerspiegelt. Een snelle en conceptueel simpele methode is om een formulering te gebruiken waarbij de dragcoëfficient lineair toeneemt met de windsnelheid tot p/m 30 m/s en daarna constant blijft.

Ondanks dat de resultaten van verschillende studies in het algemeen goed overeen komen, blijven er onzekerheden. Holthuijsen et al. (2012) vinden dat de richting van deining een grote invloed op hun resultaten heeft. Als de deining dwars of de windrichting zit vinden ze waardes voor de dragcoëfficient die tot meer dan twee keer groter zijn (bij 35 m/s) dan voor andere gevallen. Op de Noordzee komt deining voornamelijk uit het noorden, en noordelijke winden veroorzakende meest gevaarlijke situaties. Deze simpele redenering suggereert dat de door deining veroorzaakte toename van de dragcoëfficient op de Noordzee niet belangrijk is, maar de potentieel grote gevolgen vragen om nader onderzoek.

De bepaling van de windschuifspanning is een gekoppeld probleem van het lucht-water systeem. Als de dragcoëfficient afneemt, neemt de wind toe, waardoor het effect van de afnemende dragcoëfficient of windschuifspanning tegengewerkt wordt. Uiteindelijk kan het effect van een

veranderde parameterisatie van de dragcoëfficient klein zijn. Experimenten met gekoppelde modellen zijn nodig om meer duidelijkheid te verschaffen. Tot dan is het belangrijk om inconsistenties te vermijden door dezelfde dragparameterisatie in in beide modellen te gebruiken als de output van het ene (meestal wind) gebruikt wordt om het andere (bv. golven) in een ongekoppelde setting aan te drijven.

Executive Summary

The stress τ exerted by the wind on the ocean is usually parameterized as

$$\tau = \rho_a \, C_D \, U_{10}^2,$$

where ρ_a is the density of air and U_{10} the wind speed at a height of 10 m above the sea surface. C_D is the drag coefficient, which depends on the surface roughness. As the sea surface gets rougher with increasing wind speed (higher waves), the drag coefficient increases with wind speed. Usually a linear increase is assumed. There are, however, indications that the drag coefficient stops growing for $U_{10} \gtrsim 30$ m/s, and possibly decreases at even higher wind speeds.

This report reviews the post-2000 literature about the wind drag at high wind speeds. The review is grouped into observation-based studies, modelling studies that try to explain the observed behaviour of the drag coefficient, and studies in which formulations of the observed behaviour of the drag coefficient at high wind speeds are used to drive numerical wind, wave, and surge models.

The available studies that are based on *in situ* observations employ on different methods and measurement techniques to determine the drag coefficient. However, they all agree that the drag coefficient stops growing for wind speeds $\gtrsim 30$ m/s and declines for wind speeds $\gtrsim 40$ m/s. Its maximum value is $\approx (2.5 \pm 0.2) \cdot 10^{-3}$. The *in situ* results are backed by remote-sensing results from scatterometers.

The main result of the observational studies, namely that the drag coefficient levels off for wind speeds exceeding 30 m/s, can be explained theoretically by taking into account the effect of spray droplets on the atmospheric boundary layer. Furthermore, wind, wave, and surge models employing a formulation of the drag coefficient that incorporates the levelling-off result in better agreement with observations than models that do not.

The levelling-off of the drag coefficient at high wind speeds is backed by three independent lines of research. It

- is confirmed by observations using different experimental conditions and measurement techniques,
- can be explained theoretically, and
- gives better results if applied in numerical models.

This strongly suggests that the effect is real. It is therefore recommended to use a formulation of the drag coefficient that reflects the levelling-off. A quick and conceptually easy method is to use a parameterization of the drag coefficient that grows linearly with wind speed up to wind speeds of about 30 m/s and is constant for higher values.

Despite the general agreement between different studies there remain uncertainties. Especially, Holthuijsen et al. (2012) find a large impact of swell direction on their results. Under cross-swell they find drag coefficients that are more than twice as high (at 35 m/s) than in situations without cross-swell. In the North Sea swell usually travels north-south, which is also the direction of the most dangerous wind conditions. Therefore, the cross-swell enhancement of the drag coefficient might not be important for the North Sea, but its potentially large impact asks for a thorough investigation.

The determination of the surface stress is a coupled problem of the air-water system. Decreasing the drag coefficient leads to increasing wind speed, which in turn counteracts the effect of the decreasing drag coefficient on the stress. In the end the effect of changing the parameterization of the drag coefficient could be minor. Coupled model experiments are needed to shed more light on this question. In the meantime it is important to avoid inconsistencies when the winds from an atmosphere mode are used to drive a wave or a surge model in uncoupled mode. Both models should use the same drag parameterization.

1 Introduction

1.1 Scope of this report - I

The stress τ exerted by the wind on the ocean is usually parameterized as

$$\tau = \rho_a \, C_{D,z} \, U_z^2, \tag{1}$$

where ρ_a is the density of air, U_z the wind speed at a height z above the sea surface, and $C_{D,z}$ the corresponding drag coefficient. Usually, $z = 10$ m is used as the reference height, and this value is used throughout this report. For convenience, we will use the abbreviation C_D for $C_{D,10}$.

It is well-established that for low to moderate wind speeds the drag coefficient increases nearly linearly with wind speed. Its behaviour at wind speeds $U_{10} \gtrsim 30$ m/s is less well established, but the few available studies point to C_D levelling off or even dropping with wind speed at such high wind speeds.

This report reviews the existing literature about the drag coefficient a high wind speeds ($U_{10} \gtrsim 30$ m/s) and comes with recommendations on how to parametrize the $C_D - U_{10}$ at such wind speeds.

1.2 Theoretical background

The total wind stress (1) is the sum of three components, the viscous, turbulent and form stresses. At low wind speeds the sea surface is smooth, and turbulence levels are low. The total stress is dominated by molecular forces that create the viscous stress. For $U_{10} \gtrsim 5$ m/s the turbulent stress and the form stress become dominant. The form stress is due to the interaction of the air flow with the topography, here caused by waves. The turbulent stress is momentum transferred to the ocean by turbulent eddies that propagate with the mean, background wind field,

$$\tau_t = -\rho_a \overline{u'w'}, \tag{2}$$

where u' and w' are respectively horizontal and vertical velocity fluctuations, and the overbar denotes time-averaging. As the wind increases, waves are produced on the ocean surface. The surface is no longer smooth, and the interaction between airflow and waves creates the form stress.

In neutrally stable flow (no vertical acceleration) the *total* stress is constant with height in a layer close to the surface, although its three members are not. A layer of constant stress results in a logarithmic velocity profile (e.g., Tennekes 1973),

$$U(z) = \frac{u_*}{\kappa} \ln(\frac{z}{z_0}), \tag{3}$$

where $u_* = \sqrt{\tau/\rho_a}$ is the friction velocity, $\kappa = 0.41$ the von Kármánn constant and z_0 the roughness length.

Combining the logarithmic profile (3) with the definition of the drag coefficient (1) results in (remember that we use $z = 10$ m)

$$C_D = \left(\frac{u_*}{U_{10}}\right)^2 = \frac{\kappa^2}{\ln^2\left(\frac{10}{z_0}\right)}. \tag{4}$$

The roughness length is usually parameterized as

$$z_0 = 0.1\frac{\nu}{u_*} + \alpha\frac{u_*^2}{g}, \tag{5}$$

	a	b/(m/s)$^{-1}$	U_{10}-range/(m/s)
Smith and Banke (1975)	0.63	0.066	0-21
Large and Pond (1981)	0.49	0.065	11-25
Wu (1982)	0.8	0.065	0-52
Yelland and Taylor (1996)	0.60	0.070	6-26

Table 1: Results from some widely-used experimental studies. a and b are the coefficients of the linear fit (7), and the U_{10}-range is the range for which the authors state that their results are valid.

where ν is the kinematic viscosity of air, g the acceleration due to gravity, and α the Charnock parameter. The first term describes the viscous stress and is only relevant at low wind speeds.

The second term in (5) has been introduced by Charnock (1955) and describes the combined effect of turbulent and viscous stresses. Usually, α is treated as a constant. Values cited in the literature vary between 0.014 and 0.034. This large spread partly results from the fact that the roughness depends on the sea state, but that the sea state has no one-to-one relation with the wind speed. When, at a given wind speed, the waves are still growing they extract more momentum from the atmosphere than if they have reached an equilibrium (*fully developed sea*). This is the reason why ECMWF's forecast system includes a wave model. They calculate α as

$$\alpha = \frac{\hat{\alpha}}{\sqrt{1-\tau_w/\tau}}, \qquad \hat{\alpha} = 0.006, \tag{6}$$

where τ_w is the wave-induced stress that can be calculated from the wave spectrum as provided by the wave model.

1.3 Relation between C_D and U_{10}

The drag coefficient C_D depends on the surface roughness (see eq. (4)). As the sea surface gets rougher with increasing wind speed (higher waves), C_D increases with wind speed. There are, however, other factors influencing the drag coefficient at a given wind speed. Two important ones are the sea state (see (6)) and the stratification. A stable stratification suppresses turbulence and reduces the turbulent stress (2), while an unstable stratification increases turbulence and the turbulent stress. Stratification leads to deviations from the logarithmic wind profile (3). Its impact on the drag coefficient is highest at low wind speeds. To make results comparable, data are usually converted to neutral stability. All results assessed and shown in this report are for neutral stability.

Equations (3), (4) and (5) constitute implicit relations between the various variables (U_{10}, u_*, C_D, z_0) that cannot be solved explicitly. The relations have to be found experimentally. Measuring the turbulent flux (2) is challenging, especially if it has to be done on a ship. A lot of effort has been put into these measurements. After accounting for stability effects a linear relation between C_D and U_{10} is found,

$$C_D = a + bU_{10}. \tag{7}$$

Table 1 lists for some widely-used studies the coefficients a and b and the wind speed range for which they are valid. Note that most experiments were conducted in moderate to strong winds ($U_{10} \lesssim 25$ m/s). Only the study of Wu (1982) (see section 2.1) contains measurements up to 52 m/s. All his points are perfectly represented by the linear fit, and he concludes that "the Charnock relation holds even for stormy seas", but he also cautions that "this is a somewhat surprising result, the role played by sea spray on the momentum flux across the air-sea interface under these conditions still needs careful evaluation."

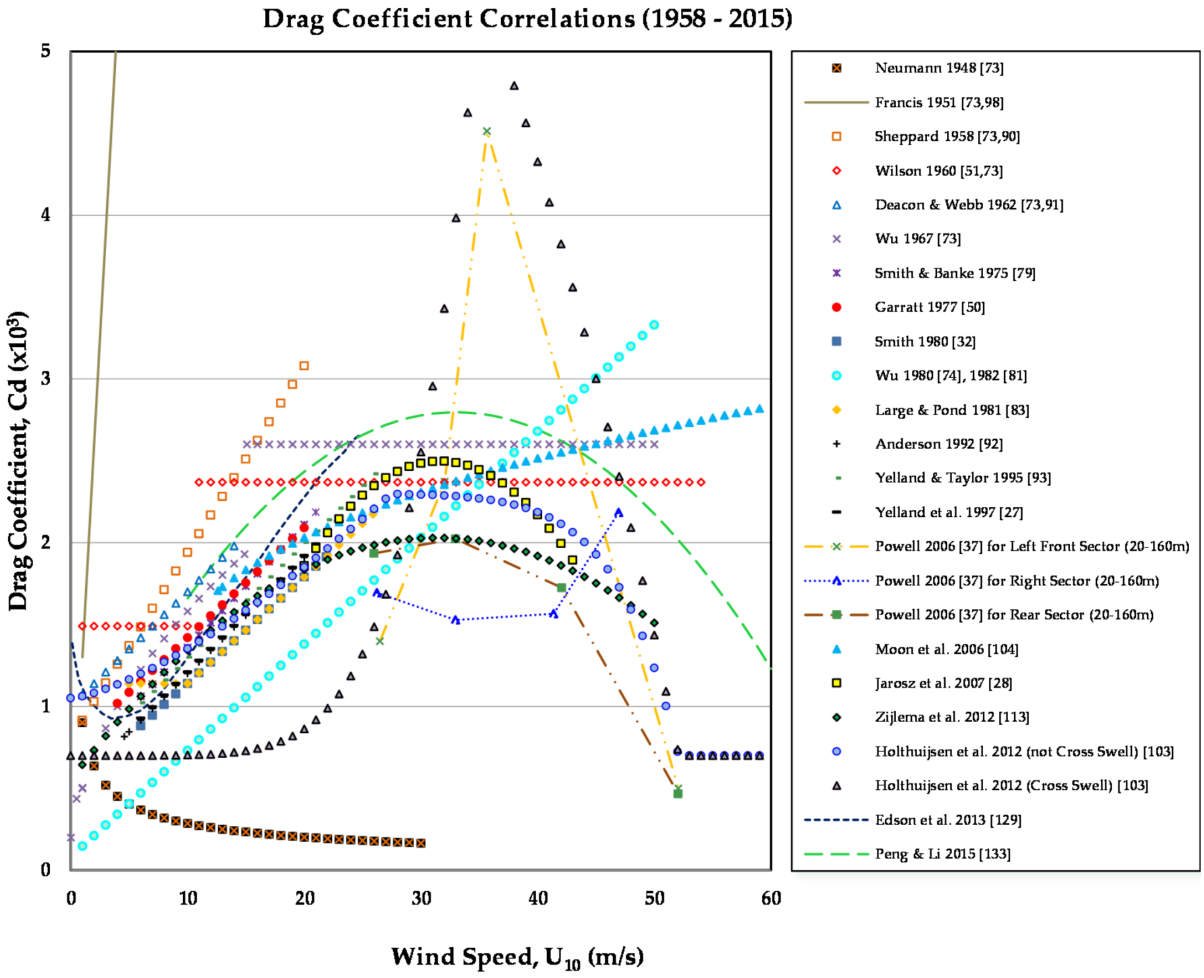

Figure 1: Drag coefficient correlations (1958-2015). (This is Figure 2 of Bryant and Akbar, 2016. For the references see that paper. Note that "Moon et al. 2006" should read "Moon et al. 2007", and "Powell et al. 2006" should read "Powell et al. 2003". Note also that the curve for the Wu (1982) fit has the wrong offset. According to Table 1 and Figure 2 the offset should be 0.8, but obviously Bryant and Akbar (2016) erroneously used 0.08 instead.)

The Wu (1982) fit is often used to translate winds into stress to drive wave or surge models. However, new (post-2000) experiments show that the drag coefficient stops growing for $U_{10} \gtrsim$ 30 m/s (levelling-off in the following), and possibly decreases at even higher wind speeds. The underlying mechanism is that at these high wind speeds a layer of droplets and foam forms a smooth surface that shields the waves from the wind. The roughness 'felt' by the wind is lower than that given by the waves. Use of the Wu (1982) parameterization thus probably leads to too high stress, and therefore to too high modelled wave or surge levels.

1.4 Scope of this report - II

In a recent paper Bryant and Akbar (2016) review the literature about drag over sea, going back to as early as Newton. They compile a large set of proposed $C_D - U_{10}$ relations and display them in one figure which is reproduced here as Figure 1. (Note that this figure contains some errors as detailed in the caption.) Most of the relations, especially the newer ones, show a decreasing of the drag coefficient for wind speeds $\gtrsim$ 30 m/s. Exceptions are the outdated studies of Wu (1967) and Wilson (1960) that argued for a constant drag coefficient, as well as those of Wu

(1982) (see section 2.1) and Moon et al. (2007) (see section 4.1). Except for the two related studies of Powell et al. (2003) and Holthuijsen et al. (2012) (see sections 2.3 and 2.4), C_D stays well below $3 \cdot 10^{-3}$ for all suggested relations.

The present report has some overlap with the Bryant and Akbar (2016) review in that it also reviews the post-2000 papers on experimental determination of the drag coefficient (section 2). It goes, however, beyond Bryant and Akbar (2016) in that it also takes into account modelling studies that try to explain the observed behaviour of the drag coefficient (section 3), and studies in which formulations of the observed behaviour of the drag coefficient at high wind speeds are used to drive numerical wind, wave, and surge models (section 4).

There appear to be four major studies on wind drag at high wind speeds based on *in situ* observations. One of them (Donelan et al., 2004) uses laboratory measurements, two employ drop-sonde measurements in hurricanes (Powell et al., 2003; Holthuijsen et al., 2012), and one (Jarosz et al., 2007) uses current measurements in the ocean underneath a hurricane. They arrive at comparable results (see Figure 1), namely that the drag coefficient

- stops growing for wind speeds $\gtrsim 30$ m/s
- slightly decreases for wind speeds $\gtrsim 35$ m/s
- reaches a maximum of $\approx (2.5 \pm 0.2) \cdot 10^{-3}$.

One study finds that the drag coefficient can be much higher under cross-swell conditions.

The results from *in-situ* measurements are backed by remote-sensing results from scatterometers (section 2.6).

The main result of the observational studies, namely that the drag coefficient levels off (or saturates) for wind speeds exceeding 30 m/s, can be explained theoretically by taking into account the effect of spray droplets on the atmospheric boundary layer. Furthermore, wave and surge models that employ a levelling-off of the drag coefficient result in better agreement with observations than models that do not.

2 Observations

2.1 Wu (1982)

Wu (1982) combines observation-based estimates of the drag coefficient from various sources, with the highest wind speed encountered being 51 m/s. He concludes that a linear relation between C_D and U_{10} (for coefficients see Table 1) "is seen to fit closely the data throughout the entire wind-velocity range" (see Figure 2).

This linear fit is widely used in wave and surge modelling. However, inspection of Wu's Table 1 shows that all data points for $U_{10} > 30$ m/s have been obtained using the momentum budget method, which is explained, e.g., in Miller (1968). It involves several approximations (e.g., that the hurricane is circular symmetric) and a vertical integral over the inflow layer. The top of this layer is where the radial velocity vanishes, but it is unclear how accurate the determination of its height is. In any case this method is less accurate than the more direct eddy-correlation method, in which u' and w' from (2) are directly measured, or the profile method, which relies on the wind measurements at different heights and their fit to the logarithmic profile (3), that are used in the papers to be discussed in the following sections.

2.2 Donelan et al. (2004)

Donelan et al. (2004) present results from laboratory (wave tank) measurements. Their results are obtained by three different methods, namely "the profile method (in which the vertical gradient of mean horizontal velocity is related to the surface stress), the Reynolds stress method, and the momentum budget or surface slope method". In the latter, use is made of the fact that the surface stress pushes the water upwind, creating a sloping surface. A careful analysis of the momentum balance of the water body leads to an expression of the surface stress in terms of the surface slope. It is worth noting that this method is totally independent of the other two (gradient and Reynolds stress). It does not involve any velocity measurements in the air, which may suffer from air-borne droplets.

Donelan et al. (2004) present their results together with laboratory results from Ocampo-Torres et al. (1994) (see Figure 3). All four data sets exhibit a remarkable agreement and show that the drag coefficient reaches a constant value of $C_D \approx 2.4 \cdot 10^{-3}$ for $U_{10} > 33$ m/s. The frequently cited drag coefficient formula of Large and Pond (1981) appears to be an upper bound for the results of Donelan et al. (2004), with the same slope for velocities $U_{10} < 33$ m/s.

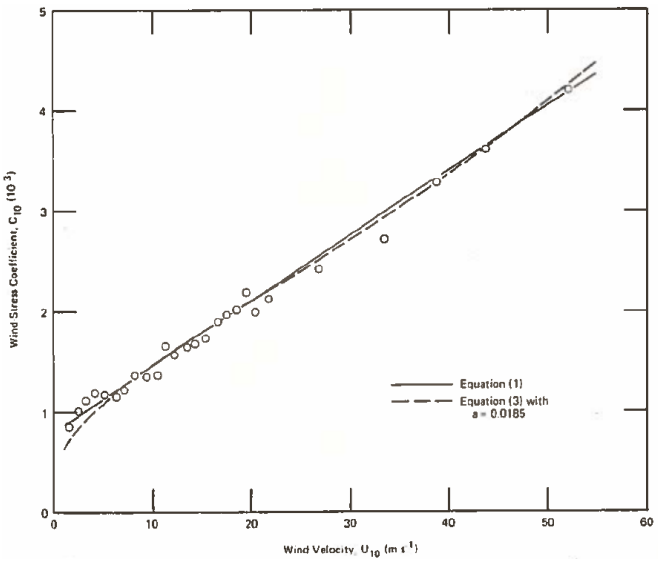

Figure 2: C_D-U_{10} relationship as found by Wu (1982). "Equation (1)" is the linear fit given by the coefficients in Table 1) . (This is Figure 1 of Wu, 1982.)

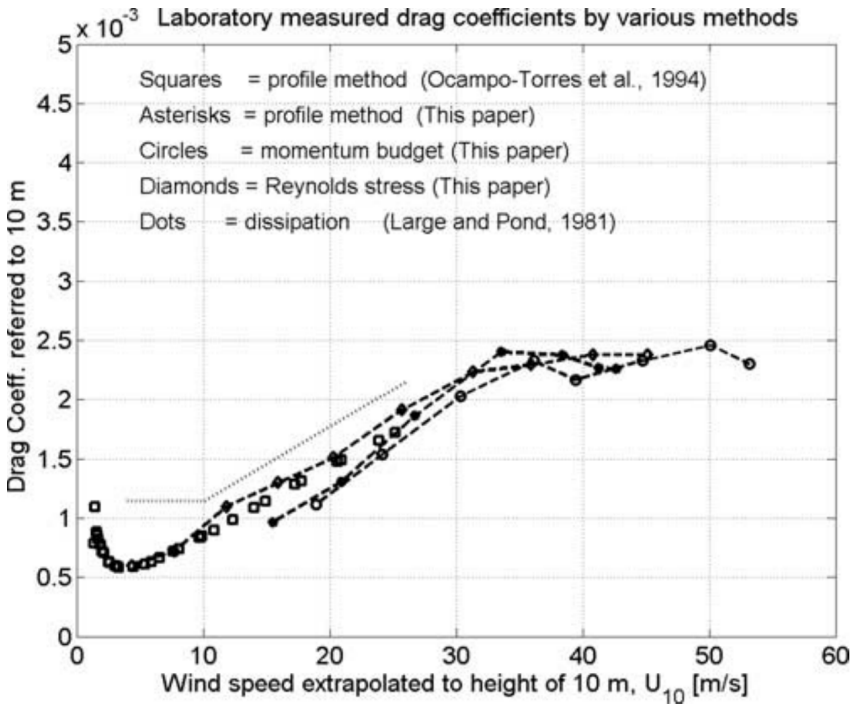

Figure 3: Laboratory measurements of the neutral stability drag coefficient by profile, eddy correlation (Reynolds) and momentum budget methods from Donelan et al. (2004). The frequently cited drag coefficient formula of Large and Pond (1981) is also shown. This was derived from field measurements. (This is Figure 2 of Donelan et al., 2004.)

The authors observe that the wind speed at which the drag coefficient becomes constant (roughly 33 m/s or Bf 12) coincides with the wind speed at which the sea surface appears completely white with foam and spray. Foam and spray are caused by breaking waves, which are much steeper than non-breaking waves. Under these circumstances the flow detaches from the surface at wave crests and re-attaches at the following one. As Donelan et al. (2004) put it, "in conditions of continuous breaking of the largest waves the aerodynamic roughness of the surface is limited, the geometric roughness of the large waves notwithstanding." Note that in this explanation of the C_D saturation the foam and spray layer does not play an active role, but only serves to signal conditions of breaking (steep) waves that lead to flow separation.

2.3 Powell et al. (2003)

Powell et al. (2003) use results from GPS drop-sondes to determine C_D. During hurricane reconnaissance flights small sondes with a GPS receiver are launched at heights between 1.5 and 3 km near the eye-wall, the region where the highest wind velocities are found. While falling the sondes transmit position and height at high frequency (every half second). From the position changes the wind speed is determined. In the lower 150 m or so the wind speeds clearly follow a logarithmic profile. Fitting the measurements to the formula for a logarithmic profile (3) yields values for u_*, U_{10} and z_0, from which the drag coefficient can be determined.

The result is shown in Figure 4. The fit to (3) is done for four height ranges (10-100, 10-150, 20-100, and 20-150 m; open symbols). The one for the 10 m-150 m range (squares) gives the smallest confidence interval. All four fits show that the drag coefficient reaches a maximum of $\max(C_D) \approx (2.5 \pm 0.3) \cdot 10^{-3}$ for wind speeds somewhere between 30 and 40 m/s, and that it declines for higher wind speeds. The largest value is found for the 20-100 m range (triangles) at $U_{10} = 40$ m/s, but with a large confidence range. While for wind speeds below 33 m/s the slope

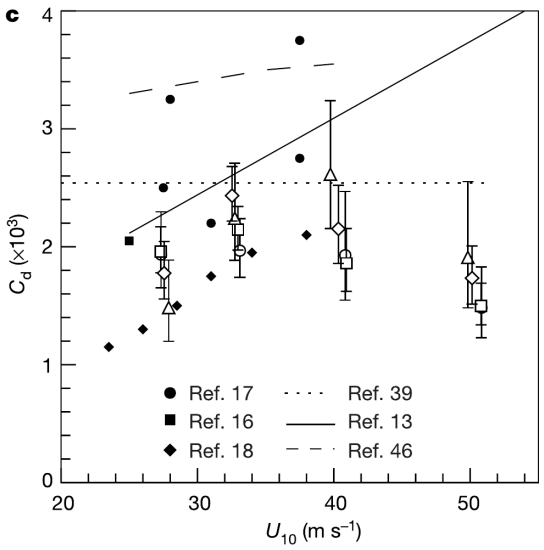

Figure 4: C_D-U_{10} relationship as found by Powell et al. (2003). The open symbols pertain to the fit to eq. (3) being done over different height ranges. The smallest error bar (95%-interval) was found for using the 10-150 m layer (squares). The figure also contains the relation of Large and Pond (1981) (solid line, "Ref. 13") and results from several other studies. (This is Figure 3c of Powell et al., 2003.)

of the $C_D - U_{10}$-line correspondents to that of the Large and Pond (1981) line, the absolute C_D values are lower.

2.4 Holthuijsen et al. (2012)

This paper employs the same method as Powell et al. (2003), but uses a much larger set of drop-sonde measurements. Therefore the authors are also able to present results for wind speeds up to 60 m/s. While Powell et al. (2003) use the 10-150 m layer to fit their measurements, Holthuijsen et al. (2012) use the 20-160 m layer. The results are presented together with those of other studies (see Figure 5), of which only those of Powell et al. (2003) (see section 2.3) and Jarosz et al. (2007) (section 2.5) contain results for $U_{10} \gtrsim 28$ m/s.

As can be seen from Figure 5, both drop-sonde based studies give similar results, which are, however, systematically lower than those of other studies, especially those of Jarosz et

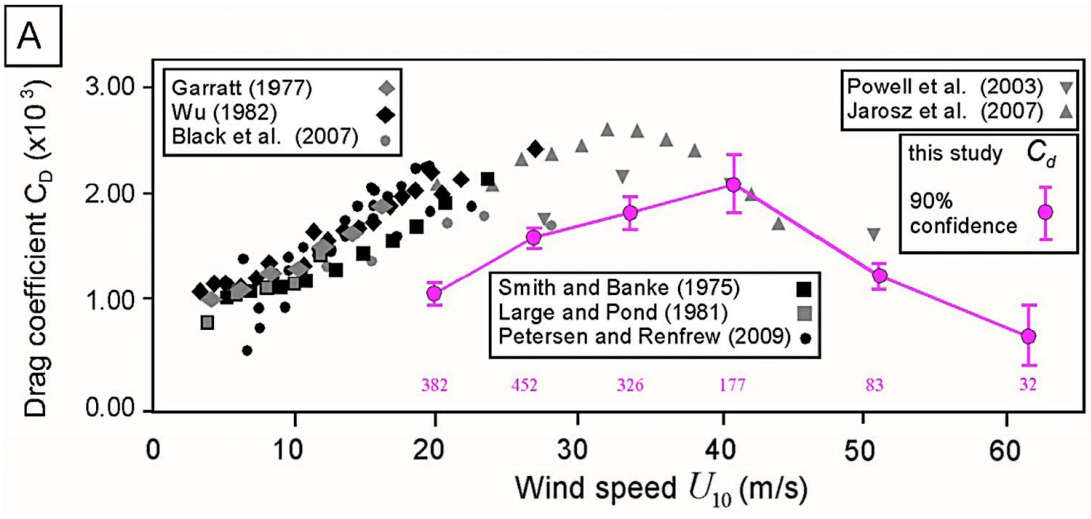

Figure 5: Bin mean values of observed drag coefficient C_D. Magenta symbols represent the C_D observation of Holthuijsen et al. (2012), while gray symbols represent observations from previous studies (indicated in insets). (This is Figure 6A of Holthuijsen et al., 2012. Note that the study of Zijlema et al. (2012) is based on this figure (cf. Figure 14).)

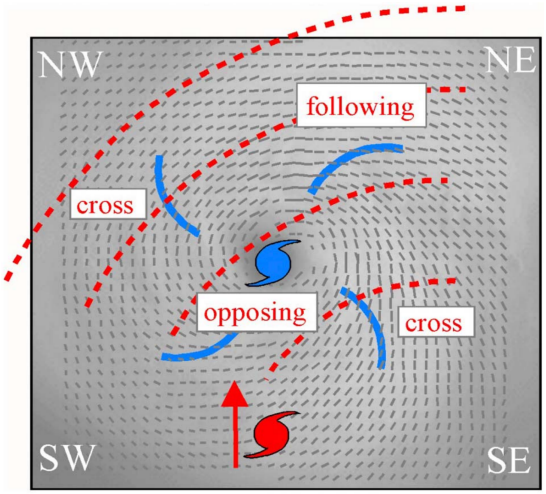

Figure 6: The swell types in a hypothetical hurricane in the Northern hemisphere moving northward. Blue symbol shows the eye. Red symbol shows the eye at a location to the south somewhat earlier in time. Blue curved lines indicate locally generated wind sea. Red curved lines indicate (young) swell generated at the southern location dispersing away from that location. Following swell occurs where red and blue lines indicate same direction of propagation (NE of eye), cross swell occurs where red and blue lines cross (NW and SE of eye) and opposing swell occurs where red and blue lines indicate opposite direction of propagation (S of eye). (This is Figure 3 of Holthuijsen et al., 2012.)

al. (2007). Holthuijsen et al. (2012) try to explain this by the effect of swell on the drag. A northward-moving hurricane contains swell that has been produced buy the same hurricane at a more southerly position earlier in time. In the left front sector of the hurricane it appears as cross-swell (see Figure 6). By sorting their data according to their position in the hurricane, Holthuijsen et al. (2012) find that for $U_{10} \lesssim 25$ m/s cross-swell reduces the drag coefficient, while it increases the drag for $U_{10} \gtrsim 35$ m/s. Sorting the earlier observations into different swell-categories, they find a large overlap with their data.

Another consequence of the swell-dependence of the drag coefficient is that for cross-swell conditions they find a drag coefficient of $C_D = 5 \cdot 10^{-3}$ at $U_{10} \approx 35$ m/s, which is more than twice as high as their average value of $\approx 2 \cdot 10^{-3}$ at this wind speed.

Holthuijsen et al. (2012) investigate the reason for the drag coefficient to stay constant or even decrease at high wind speeds. The conclude that "the levelling off of the drag coefficient and the subsequent decrease to a low limiting value coincides with the generation of streaks of foam and droplets at the surface, possibly at the expense of white caps, eventually creating white out conditions at $U_{10} > 40$ m/s." The layer of foam and droplets forms an aerodynamically "smooth" surface that decouples the atmosphere from the "real" ocean surface.

2.5 Jarosz et al. (2007)

Usually, stress and drag are determined from measurements in the atmosphere. The stress is obtained by extrapolating wind speed measurements to the surface, assuming a logarithmic profile. Jarosz et al. (2007) use a different approach. They determine the stress by considering the momentum balance in the water, assuming a barotropic initial response. A justification of this assumption and the derivation of the balance is given in the supporting online material (`www.sciencemag.org/cgi/content/full/315/5819/1707/DC1`). The balance reads

$$\frac{\partial U}{\partial t} - fV = \frac{\tau_{sx}}{\rho H} - \frac{rU}{H}, \tag{8}$$

where ρ is a reference density (1025 kg m^3), f is the Coriolis parameter ($0.71 \cdot 10^4 s^{-1}$), U and V are the depth-integrated along-shelf and cross-shelf velocity components, respectively, H is the water depth, r is a constant resistance coefficient at the sea floor, and τ_{sx} is the along-shelf wind

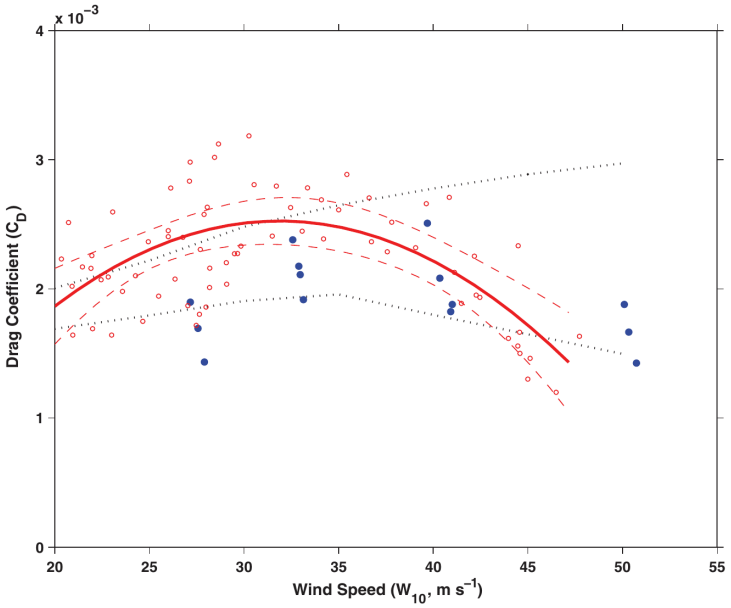

Figure 7: Drag coefficient as a function of wind speed from Jarosz et al. (2007). C_D is shown for an observation-based resistance coefficient, $r = 0.02$ cm/s. The red open circles are the evaluated C_D from the current and wind observations, the solid red line is a fitted quadratic curve to the C_D estimates, and the red dashed lines are the 95% confidence limits for this quadratic curve. The black dotted lines represent the window for C_D reported in Moon et al. (2004), whereas the blue dots represent C_D reported in Powell et al. (2003). (This is Figure 3 of Jarosz et al., 2007.)

stress, which is written in the usual way as $C_D U_{10}^2$. Inserting this expression into (8) results in an expression for C_D.

U_{10}, U and V are measured by buoys and moored current meters that where passed by hurricane Ivan in 2004. For all values of the resistance parameter r the best fit to the data is obtained by a quadratic fit between C_D and U_{10}. The maximum of the drag coefficient is at about 32 m/s, where a value of $r = 0.02$ cm/s for the resistance parameter yields $C_D = (2.5 \pm 0.2) \cdot 10^{-3}$. The value for r is chosen to obtain results consistent with those of Moon et al. (2004) and Powell et al. (2003) (see Figure 7).

That a different method to determine the stress than earlier studies leads to the same qualitative behaviour of the $C_D - U_{10}$ relation, i.e., the existence of a maximum for $U_{10} = 30 - 35$ m/s, gives confidence in this result. The absolute value of C_D, however, is determined in order to have results comparable to other studies by choosing a particular value for r. Higher (lower) values for r will result in higher (lower) values for C_D.

2.6 Scatterometers

Scatterometers measure the backscatter of microwaves from the ocean surface. The backscatter increases with roughness and thus wind speed. The precise relation between backscatter and wind speed ("Geophysical Model Function" - GMF) is determined statistically by fitting the measured backscatter signal to collocated wind speeds from buoys and the ECMWF model (e.g., Hersbach et al., 2007). In the same way a relation between backscatter and stress can be constructed (Portabella and Stoffelen, 2009).

Measurements from aircraft-based scatterometers at moderate to high high wind speeds (25-65 m/s) show that the backscatter "stops increasing at hurricane-force winds" (Fernandez

et al., 2006). This indicates that the roughness does not increase further with increasing wind speed, in line with the results from the *in-situ* observations summarized above. The figures shown in Fernandez et al. (2006) show a constant backscatter signal above $\approx$ 40 m/s, and a clear reduction in increase above $\approx$ 30 m/s.

2.7 Discussion

The four major studies that are based on *in-situ* observations employ different and independent methods to determine the drag coefficient. One (Donelan et al., 2004) uses laboratory measurements and three different methods to determine the drag coefficients. Two of them involve velocity measurements in air, and one relies on the measurement of the stress-induced slope of the air-water interface. The results from all three methods agree well with each other and with results from an earlier wave-tank study by a different group (Ocampo-Torres et al., 1994).

The other three studies are based on measurements in real hurricane conditions. Two of them (Powell et al., 2003 and Holthuijsen et al., 2012) rely on wind measurements by drop sondes in hurricanes, while the third exploits the effects of the hurricanes on the water movement. Despite these differences in method, their results are comparable and agree with those of the wave-tank measurements.

Figure 5 contains the results of three of the four studies. Not surprisingly given the overlap in data and authorship, Powell et al. (2003) and Holthuijsen et al. (2012) arrive at identical results. However, for $U_{10} < 40$ m/s their C_D-values are substantially lower than those of Jarosz et al. (2007), and lower than those of earlier studies for moderate wind speeds. A comparison with Figure 3 shows that also the results of Donelan et al. (2004) are higher than those of Holthuijsen et al. (2012). Taken together, these results give the impression that the results of Holthuijsen et al. (2012) and Powell et al. (2003) are too low. Holthuijsen et al. (2012) try to explain the discrepancy by the swell-dependence of C_D, noting that under cross-swell their C_D-values can be more than twice as high than the values shown in Figure 5. More research is needed to resolve this question.

Despite the discrepancy that they find in the magnitude of the drag coefficient, all studies agree that C_D reaches a maximum for U_{10}-values somewhere between 30 m/s and 40 m/s. From Figures 5 and 3 an upper bound for the maximum is $C_{D,max} = (2.5 \pm 0.2) \cdot 10^{-3}$. Note that this value is an average over a large number of individual values. Individual values can be much higher.

Holthuijsen et al. (2012) provide evidence for swell direction systematically influencing the drag coefficient in hurricanes. Independent studies are needed to confirm this effect. Furthermore, its importance for the North Sea needs investigation. Swell enters the North Sea from the North Atlantic north of Scotland and travels southward, and the most dangerous wind situations in the North Sea occur with northerly winds, which implies wind and swell to be parallel. While this simple reasoning implies only a small role for potential cross-swell enhancement of the drag coefficient in the North Sea, its potential effects of more than a doubling of the drag coefficient are large.

The various studies reviewed find a maximum values for the drag coefficient of $C_{D,max} = (2.5 \pm 0.2) \cdot 10^{-3}$. The Wu (1982) parameterization yields a value of $C_D = 2.75 \cdot 10^{-3}$ at $U_{10} = 30$ m/s. A 'capped Wu' parameterization in which the drag coefficient follows the Wu (1982) parameterization up to $U_{10} = 30$ m/s and remains constant for higher wind speeds provides a good upper bound for the drag coefficient.

The main result of the aforementioned studies, i.e., that the drag coefficient does not increase for wind speeds beyond 30 m/s, is confirmed by totally independent scatterometer measurements. They show that the backscatter, which is a measure of surface roughness and thus stress, does not increase for wind speeds $\gtrsim$ 30 m/s.

2.8 Summary and conclusion

The results form the observational studies can be summarized as follows

- as a function of the 10-m wind speed, the drag coefficient reaches a maximum of $C_{D,max} = (2.5 \pm 0.2) \cdot 10^{-3}$ between 30 m/s and 40 m/s,
- this maximum corresponds to the value that the Wu (1982) parameterization attains at ≈ 30 m/s,
- the Wu (1982) parameterization, capped at its value at 30 m/s, gives an upper bound for the drag coefficient,
- the impact of swell on the drag coefficients needs further investigation.

3 Theoretical explanations

Attempts to explain the levelling-off of the drag coefficient as function of the wind speed invoke one or more of the following effects,

- air-flow separation - at high wind speeds and large wave heights, the air flow cannot follow the sea surface any more. It detaches behind a wave crest and re-attaches at the following crest. Therefore, the air flow does not "feel" the actual roughness of the sea surface.
- spray/foam layer - at high wind speeds the whole sea surface is covered by a layer of foam and spray droplets ('white out'). This layer is smoother than the actual sea surface.
- falling droplets - while falling back to the surface, spray droplets transport momentum downward, increasing the wind speed close to the surface. As a result, the vertical wind shear is reduced, the vertical momentum transport is suppressed and the drag coefficient does not grow.

3.1 Bye and Jenkins (2006)

Bye and Jenkins (2006) develop a theory of the momentum flux across the air-sea interface in which they take into account that there is not only a *downward* momentum flux in the atmosphere, but also an *upward* one in the ocean as the velocity of the wave-orbital motion is larger at the surface than below it (inertial coupling relation; Bye and Wolff, 2004). The net momentum transport across the interface is the difference between these two contributions. The resulting expression for C_D is fitted to the observational data of Powell et al. (2003) (four points representing wind speeds between 30 m/s and 60 m/s) plus data from the JASIN (Joint Air-Sea Interaction) study (Nicholls, 1985) representing much lower wind speeds (7.5 m/s). The best fit exhibits a maximum of $1.99 \cdot 10^{-3}$ at $U_{10} = 42$ m/s, but the maximum is very broad with C_D values being nearly constant above 30 m/s.

Bye and Jenkins (2006) explain their results in terms of spray that is torn off from breaking waves at high wind speeds, forming a "slip" surface at the sea surface. The wind feels a smoother surface than the actual air-water interface. For the peak of the drag coefficient they find that just above one quarter of the work exerted by the wind on the water is used for spray production, and three quarters for wave growth. A model that explicitly accounts for spray droplet production yields a form of the $C_D - U_{10}$ relation that resembles the fit found from their inertial coupling model. This finding backs their idea of spray production being the reason behind the constant drag coefficient at very high wind speeds.

It should be stressed that the precise form of their $C_D - U_{10}$ relation, especially the location of its maximum, depends on their fit to the Powell et al. (2003) data. Thus the absolute value they find for the maximum C_D is no independent information. However, the fact that their theory predicts the existence of a maximum (before fitting to data) backs the observational results discussed in section 2.

3.2 Makin (2005)

Makin (2005) explains the reduced drag by an increase of air velocity near the surface that is caused by falling spray droplets. They transport momentum downward, increasing the air velocity, but cannot transfer the momentum to the sea surface because the lift created by the strong velocity shear near the surface keeps them floating. In a way the droplet-laden layer is stratified and the turbulence suppressed. Based on these assumptions, Makin (2005) arrives at the following formulation for the wind profile (his eq. (7))

$$u(z) = \frac{u_*}{\kappa\omega} \ln(\frac{z}{z_0^l}), \tag{9}$$

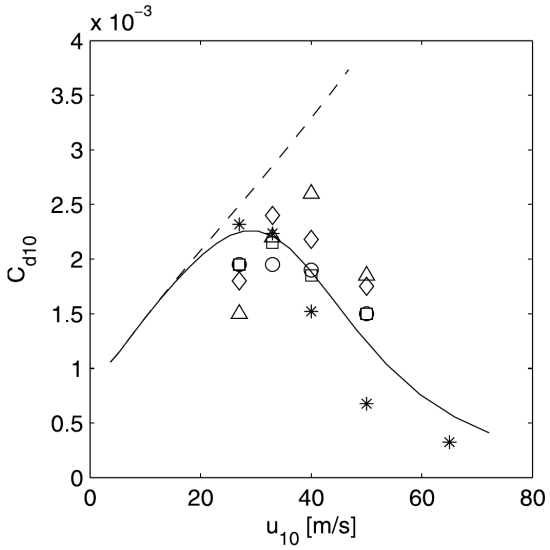

Figure 8: Drag coefficient C_D versus wind speed at 10 m height. Dash lines are reference calculations (no effect of sea drops) for the Charnock roughness scale (second term of (5)). Solid lines are model calculations corresponding to the roughness scale which accounts for the effect of sea drops according to Kudryavtsev (2006). Open symbols are data taken from Powell et al. (2003) (their Figures 3a and 3c). Stars are estimates of C_D derived by Kudryavtsev (2006) based on an assumption of the Ekman part of the atmospheric boundary layer and the profiles given in Figure 2 of Powell et al. (2003). (This is Figure 9a of Kudryavtsev, 2006.)

with the roughness length (his eq. (11b)),

$$z_0^l = c_l^{(1-1/\omega)} c_{z_0}^{1/\omega} \frac{u_*^2}{g}, \tag{10}$$

where c_l is of order 10, and c_{z_0} is the Charnock constant (α in (5)). The impact of the droplets on the airflow is described by $0 \leq \omega = \frac{a}{\kappa u_*} \leq 1$, a being the terminal fall velocity of the droplets. For $\omega = 1$ there is no impact, and (9) and (10) reduce to the usual logarithmic wind profile (3) and Charnock relation (5), respectively. In this case the turbulent velocity fluctuations are large enough to keep the droplets floating in the air ($u_*^2 \sim < u'w' >$). Otherwise the droplets are falling and transport momentum downward, increasing the velocity near the surface.

Makin (2005) notes that although c_l in (10) is only poorly defined, its actual value has only a very small impact on the resulting drag coefficient. Estimating ω from the measured friction velocities of Powell et al. (2003) and assuming droplet radii of about 80 μm, Makin (2005) arrives at a $C_D - U_{10}$ curves that is in good agreement with that of Powell et al. (2003). Note that this agreement is because ω has been chosen accordingly. However, the fact that there is a levelling-off of the drag follows from the theory, and the parameter values to be chosen to fit the data are reasonable.

3.3 Kudryavtsev (2006)

Kudryavtsev (2006) starts from the same model of droplets influencing the air flow as Makin (2005). He gives a complete derivation of (9). While Makin (2005) takes the presence of droplets as given, Kudryavtsev (2006) investigates their origin. He finds that droplets ejected vertically from bursting bubbles do not give an effect large enough to explain the observed levelling-off. However, if he assumes that the droplets are horizontally torn off from breaking waves, he is able to derive an expression for the drag coefficient that for observed droplet production rates results in values that are in good correspondence with observed ones, especially those of Powell et al. (2003). His results are shown in Figure 8.

3.4 Kudryavtsev and Makin (2011); Kudryavtsev et al. (2012)

Makin (2005) and Kudryavtsev (2006) consider the suppression of the turbulent mixing due to the effect of droplets on the atmospheric stratification. Kudryavtsev and Makin (2011) extend

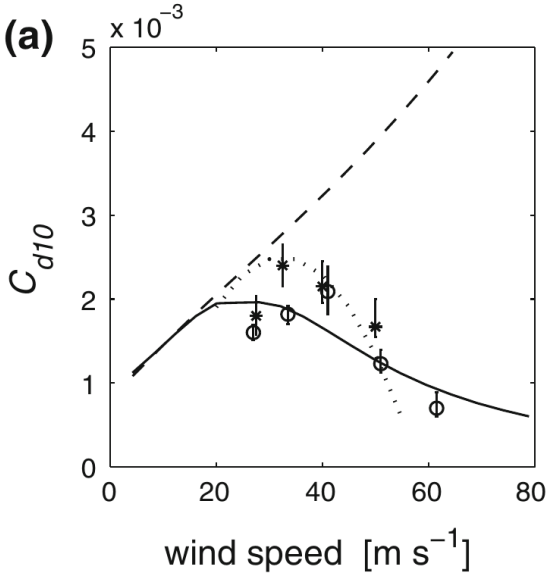

Figure 9: As Figure 8, but for the drag coefficient as derived by Kudryavtsev and Makin (2011) (black line). The dotted line represents a quadratic fit to the Jarosz et al. (2007) data. (This is Figure 7a of Kudryavtsev and Makin, 2011.)

this work by accounting for the mass of the droplets, i.e., including the mass of the droplets in calculating the density of the air-droplet mixture. This leads to the introduction of a particle force, i.e., the force needed to accelerate the droplets when they move vertically. Kudryavtsev and Makin (2011) find that the particle force is dominating the stratification effect. They are able to derive an expression for the drag coefficient that, with reasonable choices for some free parameters, fits the Powell et al. (2003) data (see Figure 9) well.

In a follow-up paper Kudryavtsev et al. (2012) derive a simplified parameterization of the drag coefficient found by Kudryavtsev and Makin (2011). Furthermore, they extend the theory to the bulk-transfer coefficient for sensible and latent heat, which are found to increase due to the presence of droplets. As a result, the ratio of the exchange coefficient C_E for enthalpy (sensible + latent heat) and momentum C_D increases, exceeding the critical value of 0.75 that was found to be necessary for the development of tropical cyclones by Emanuel (1995). For lower values of the C_E/C_D ratio the cyclones would lose more energy due to the drag than they gain through latent heating and would die out.

3.5 Richter and Sullivan (2013)

While Makin and Kudryavtsev (see above) try to find an analytical solution for the momentum transport at the sea surface, Richter and Sullivan (2013) employ direct numerical simulation (DNS) in an idealized setting (Couette flow). They find that particles tend to stabilize the atmospheric boundary layer and thus reduce the *turbulent* stress. However, this effect is largely compensated for by the particle stress, so that the *total* stress remains nearly constant. They conclude that aerodynamic effects are the cause of the C_D saturation rather than the interaction with particles. They do not specify the nature of these aerodynamic effects.

This result is at odds with that of Kudryavtsev and Makin (2011), who find that the *total* drag coefficient levels off and decreases at higher wind speeds. There are several possible reasons for this discrepancy, namely

- the effect of the direction in which droplets are torn off the breaking waves (Kudryavtsev, 2006) is not taken into account by Richter and Sullivan (2013)
- Druzhinin et al. (2017) show that the velocity at which the particles are ejected plays an important role. This is not accounted for by Richter and Sullivan (2013)

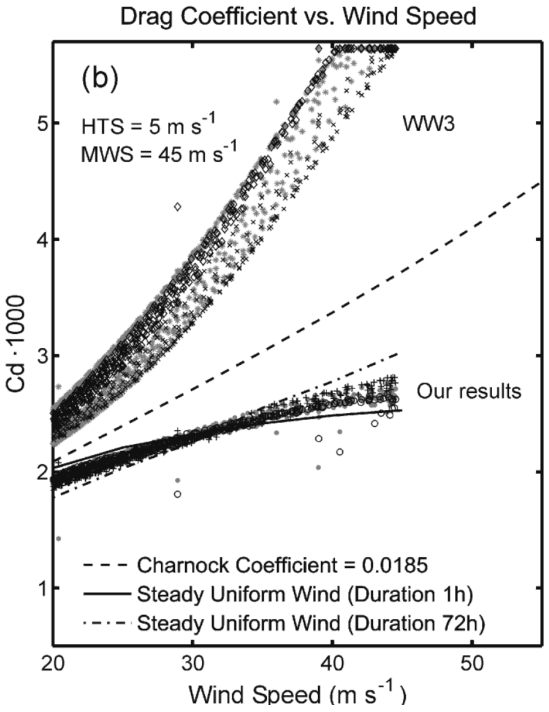

Figure 10: Scatterplot of C_D as function of the wind speed in all grid points for a storm with a translation speed of 5 m/s. The solid line and dashed-dotted line represent results obtained without incorporating the high-frequency tail of Hara and Belcher (2002) at 1 and 72 h after the onset of the steady uniform wind, respectively. The dashed line is the bulk formula based on a Charnock parameter of $\alpha = 0.0185$. The results of Moon et al. (2004) and WW3's prediction are plotted using different symbols according to the relative position from the storm center (right-front quadrant: plus, cross; left-rear quadrant: circle, diamond; other quadrants: bullet, star). (This is Figure 6b of Moon et al., 2004.)

- Richter and Sullivan (2013) perform their calculation for a Reynolds number of 8100. As usual for Couette flow, they base their Reynolds number on the thickness H of the fluid layer and the velocity difference U_0 across that layer: $Re = U_0 H/\nu$. For $\nu = 1.5 \cdot 10^{-5} \mathrm{m}^2/s$ (kinematic viscosity of dry air at 15°C) we find that $U_0 = 30$ m/s corresponds to $H \approx 4$ mm. This value is very low and cannot be meaningfully associated with the thickness of the foam layer which is several tens of centimeters thick. It seems that the chosen value of the Reynolds number is too low to adequately describe the marine boundary layer at high wind speeds.

- Neither of the papers mentioned takes the effect of the waves into account: the surface is not flat, and its topography moves relative to the air. Druzhinin et al. (2017) show that the presence of waves has an impact on the effect of droplets on the drag, the key parameter being the wave steepness. Druzhinin et al. (2017) use a Reynolds number of 15,000, still too low to properly describe the marine boundary layer.

3.6 Moon et al. (2004)

Moon et al. (2004) investigate the effect of wind-wave coupling on the air-sea stress. They combine wave spectra as produced by the Wavewatch III (WW3) wave model with the spectral tail as derived by Hara and Belcher (2002) and incorporate it into the wave boundary layer model of Hara and Belcher (2004). As a result they are able to "explicitly calculate the wave-induced stress vector, the mean wind profile, and the drag coefficient over any given complex seas". They present results for wind speeds up to 45 m/s (see Figure 10). Their drag coefficients are much lower than those resulting from WW3 alone, and lower than those using a Charnock formulation with a constant Charnock parameter. However, although their drag is lower than that from the Charnock parameterization, it does not level off but keeps growing until their maximum wind speed of 45 m/s.

From their observations both Donelan et al. (2004) and Holthuijsen et al. (2012) conclude that the forming of foam and spray must play a role in the levelling-off of the drag coefficient. It is therefore interesting to note that the model of Moon et al. (2004) does not involve any effect of

spray or foam on the momentum exchange, but is based solely on the interaction between waves and air flow. This may explain why they only find a reduction in growth with wind speed, but no levelling-off of the drag coefficient. This indicates that both processes, wind-wave interaction and the forming of spray droplets, may act together to produce the observed levelling-off.

3.7 Summary and conclusion

Models of the atmospheric boundary layer that take into account the interaction between airflow and spume droplets torn off from breaking waves can explain the observation that the drag coefficient levels off at high wind speeds (30 m/s or so) and decreases at even higher speeds. The precise positions of the maximum and the absolute level of the $C_D - U_{10}$ relation depend on parameters that are not well-constrained by observations (e.g., droplet radii), but good fits to the observations are achieved for reasonable values of these parameters. This lends credit to the validity of these models.

A model that solely relies on wave-wind interaction (Moon et al., 2004) produces substantially lower drag values than the classical Charnock relation, but shows no sign of levelling-off. This probably indicates that both processes, wave-wind interaction and foam forming, are together responsible for the levelling-off.

At the moment DNS is not able to reproduce the observed levelling-off of he drag coefficient, presumably due to too a low value of the Reynolds numbers employed. The simulations do, however, show that the form of the air-sea interface (wavy or not) has a profound impact on the impact of the spray droplets on the air flow. Position and velocity of the droplets injected into the air are also important parameters that can change the results. Without knowing these parameters from observations no firm conclusions can be drawn from DNS.

Together, there are several explanations for the levelling-off of the drag coefficient. At the moment it is not clear which of them is the most important one. Probably they all contribute in one way or another to the observed effect. However, they all indicate a levelling-off above roughly 30 m/s, thus backing the conclusions drawn from observation-based estimates of the drag coefficient.

4 Modelling

Several authors report better model performance when they employ drag-wind parameterizations that result in a maximum value for the drag coefficient than they obtain for unlimited drag values. This applies to wave and surge models as well as to hurricane forecasts.

4.1 Moon et al. (2007)

The paper is based on the results of Moon et al. (2004). A fit of those results for $U_{10} > 12.4$ m/s yields a linear relation between roughness length and U_{10}, and a quadratic one between roughness length and friction velocity. Although C_D keeps growing for wind speeds beyond 30 m/s, it shows a good correspondence with the Powell et al. (2003) data up to 40 m/s, and it is compatible with a Wu (1982) parameterization that is capped at $C_D = 2.5 \cdot 10^{-3}$.

Using the new parameterization to re-forecast several hurricanes results in a better correspondence with observations than the parameterization used operationally at the time of writing the paper. As Figure 11 shows, high wind speeds, although improved with respect to the operational parameterization, are still underestimated. It is tempting to ascribe this to the fact that C_D is still rising at high wind speeds.

4.2 Walsh et al. (2010)

Walsh et al. (2010) drive an ocean model with winds representing different tropical cyclones and wind speeds up to 80 m/s. The wind fields were derived from observed central and environmental pressures and an estimate of the observed radius of maximum wind using the simple model of Holland (1980). In translating the wind into stress to drive the ocean model, the parameterizations of Jarosz et al. (2007), Donelan et al. (2004) and Large and Pond (1981) are used. Model results are validated against sea surface temperature (SST) observations. It is found that using the drag relation based on Jarosz et al. (2007) leads to the best results, while the Large and Pond (1981) parameterizations yields the worst ones. The stress is too high, leading to too much vertical mixing in the ocean and consequently to too much cooling. Consistent with this result the Donelan et al. (2004) parameterization with values of the drag coefficient between those of the two other parameterization at high wind speeds resulted in SST cooling in between those from the other parameterizations.

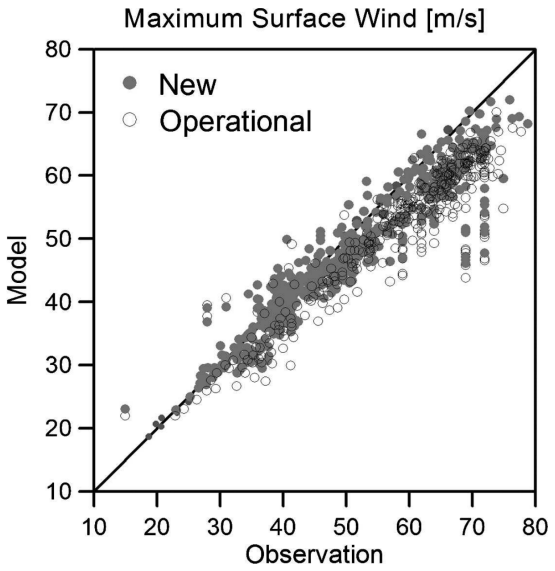

Figure 11: Comparison of the maximum surface wind between models and observations during 11 forecasts of Hurricanes Isabel (2003), Ivan (2004), Frances (2004), Charley (2004), and Jeanne (2004). Open circles are from the operational model and filled circles are from the new formula. (This is Figure 9 of Moon et al., 2007.)

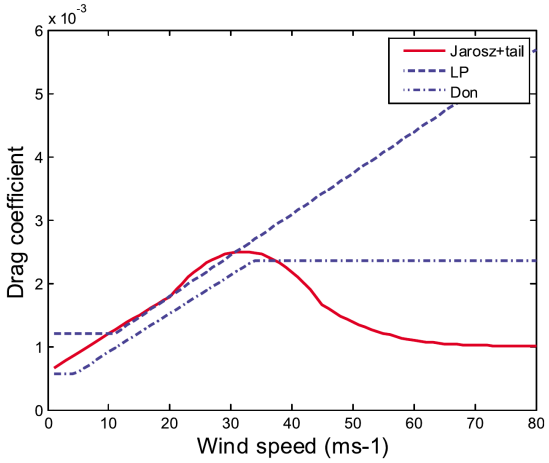

Figure 12: Assumed form of drag coefficient versus 10 m wind speed, following Jarosz et al. (2007) but extended by a tail, compared with those proposed by Large and Pond (1981) and Donelan et al. (2004). (This is Figure 3 of Walsh et al., 2010.)

4.3 Zweers et al. (2010, 2015)

Zweers et al. (2010) perform simulations of hurricanes Ivan (2004) and Katrina (2005), using the high-resolution limited area model HIRLAM. The model is still used operationally at KNMI. The simulations are done for two parameterizations of the drag coefficient. The first one employs a Charnock relation with a constant Charnock parameter of 0.025, while the second one is based on the work of Makin (2005) (see sec 3.2). The $C_D - U_{10}$ relations for both parameterizations are shown in Figure 13.

The forecasts with the new parameterization give better correspondence with observations than those using the constant Charnock parameter. Wind speeds get higher and core pressures lower. For example, wind speed and core pressure in the 96 h-forecast for Katrina reach 57 m/s and 906 hPa, respectively, for the constant Charnock case, but 98 m/s and 872 hPa, respectively, for the new parameterization.

In a follow-up study Zweers et al. (2015) repeat the simulations of Zweers et al. (2010), but instead of the Makin (2005) parametrisation of the drag coefficient that of Kudryavtsev et al. (2012) is used, and also the exchange coefficient for enthalpy is modified according to that paper. The authors conclude that their "simulations show that realistic tropical cyclone wind speeds and central pressure can be obtained with the proposed drag and enthalpy parametrizations". In addition they find a strong impact of SST and wind-induced SST *changes* on their results, calling for a coupled (atmosphere + ocean) modelling approach for tropical cyclones.

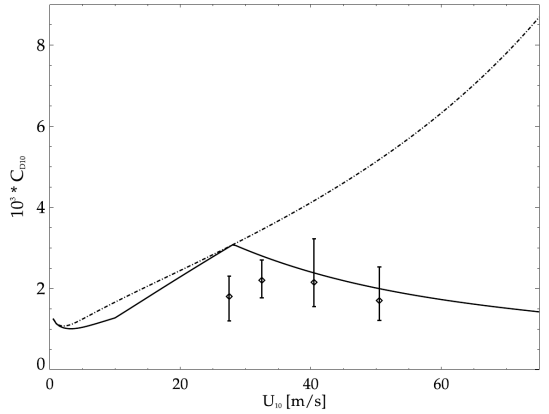

Figure 13: The drag coefficient at 10-meter height as a function of 10-meter wind speed, for the common Charnock relation (dasheddotted line) and the new drag parameterization based on Makin (2005) (solid line). Observational data by Powell et al. (2003) are indicated by diamonds. (This is Figure 1 of Zweers et al., 2010.)

4.4 Vatvani et al. (2012)

A coupled wave-surge model (SWAN + Delft3D) is forced by four different wind–drag coefficient combinations during hurricanes Ivan (2004) and Katrina (2005). Next to observed winds also the model-generated winds of Zweers et al. (2010) (section 4.3) are used. The wind data are combined with the standard Charnock parameterization of the drag coefficient (denoted as "Charnock" in the following) as well as with the Makin (2005) based formulation of Zweers et al. (2010) that is displayed in Figure 13 (denoted as "Makin" in the following). The four combinations to force the coupled wave-surge model are

- observed winds + Charnock
- observed winds + Makin
- HIRLAM winds simulated using Charnock (HIRLAM-1) + Charnock
- HIRLAM winds simulated using Makin (HIRLAM-2) + Makin

It is found that storm surges are overestimated when the parameterization with a constant Charnock parameter is used. While this could be expected for the observed wind case, it also occurs when the HIRLAM-1 forcing is used. Although the HIRLAM-1 wind speeds are lower than the observed winds, the use of the high Charnock C_D-values results in too high stress. The best results are obtained if the Zweers et al. (2010) parameterization for the drag coefficient is used to drive the storm surge model. For the wave model, no significant impact of the different wind-drag combinations is found. However, the influence of the waves on storm surge levels is found to be significant.

4.5 Zijlema et al. (2012)

Common practise in wave modelling is to use different values for the bottom drag coefficient for wind sea and swell waves, respectively. Zijlema et al. (2012) realize that the origin of this discrepancy might be that the high value for wind sea was obtained under strong wind conditions using a wind drag coefficient that was too high. They compile a set of observation-based drag coefficients (mainly those discussed in section 2) at high wind speeds and fit a quadratic curve through these values (see Figure 14).

Zijlema et al. (2012) investigate the impact of their quadratic fit in the SWAN wave model (see `http://swanmodel.sourceforge.net/online_doc/swantech/node15.html`), which employs the Wu (1982) parameterization as default (also indicated in Figure 14). They find that their parameterization together with one single value of the bottom friction coefficients for wind sea and swell gives essentially the same results as the Wu (1982) parameterization and two distinct values for bottom friction. As their fit better represents the observations (see Figure 14), they recommend its use together with one single value for the bottom friction.

4.6 Summary and conclusions

When applied in wave, surge and hurricane models, drag formulations for which he drag coefficient levels off or even declines at high wind speeds perform better than those using a linear $C_D - U_{10}$ relation. The studies of Moon et al. (2007) and Walsh et al. (2010) contain evidence that a declining drag coefficient improves results compared to a constant one. The modelling studies thus support the findings of the observational studies discussed in section 2.

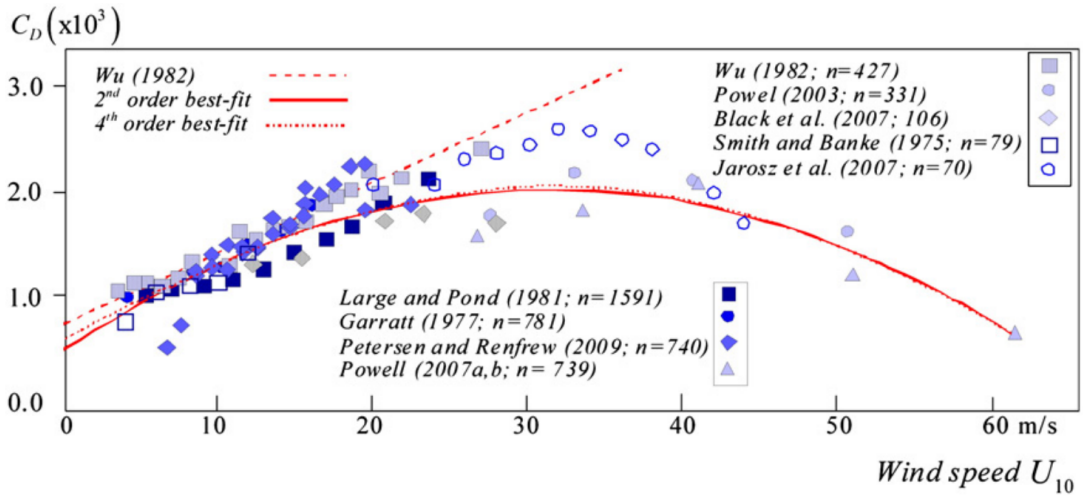

Figure 14: Observed values of the wind drag coefficient C_D from various studies and the weighted best-fit 2nd- and 4th-order polynomial (n is the number of independent data points per study). Note that this figure is based on Figure 5. (This is Figure 3 of Zijlema et al., 2012.)

5 Conclusion

We have reviewed the literature on observations of wind drag coefficients at high wind speeds, theoretical models to explain the observations, and the impact of employing them in wind, wave and swell models. These three lines of investigation give a coherent picture. The observed levelling-off of the drag coefficient for wind speeds $\gtrsim 30$ m/s can be explained theoretically, and employing a levelling-off drag coefficient in numerical models results in a better performance of the models. The majority of the studies even favours a decline of the drag coefficient for wind speeds $\gtrsim 35$ m/s.

Based on this evidence it is recommended to use a $C_D - U_{10}$ relation in which the drag coefficient does not increase for wind speeds $\gtrsim 30$ m/s. For smaller wind speeds the parameterization of Wu (1982) can be used. At $U_{10} = 30$ m/s this parameterizations gives a drag coefficient of $2.75 \cdot 10^{-3}$, which is an upper limit for the observed drag coefficients. A 'capped Wu' parameterization (linear up to 30 m/s, constant for higher winds) is thus an easy first step to take the results reviewed in report into account. In a second step the use of parameterizations that have C_D declining for high wind speeds, e.g., the parabolic one of Zijlema et al. (2012), should be investigated.

Two (though not independent) studies revealed a large enhancement of the drag coefficient in the presence of cross-swell. This aspect clearly deserves more attention. Besides the question whether the effect is real or some artefact of the data analysis, its potential impact on the North Sea needs further investigation. Swell enters the North Sea from the North Atlantic north of Scotland and travels southward, and the most dangerous wind situations in the North Sea occur with northerly winds, which implies wind and swell to be parallel. While this simple reasoning implies only a small role for potential cross-swell enhancement of the drag coefficient, its potential effects of more than a doubling of the drag coefficient are large. Therefore, the importance of swell on C_D in the North Sea needs to be investigated.

Finally, it should be kept in mind that the drag between ocean and atmosphere is a coupled problem. Reducing the drag increases the wind speed. The change in stress is given by the product of these two changes (see (1)). In the end the effect of employing a different formulation of the drag coefficient might be small. For instance, Van den Brink et al. (2013) find that the relative change in stress is only half of that in C_D, and the resulting impact on wind speed is less than 25%. Zweers et al. (2012) find that a similar relation between the relative changes in C_D and stress, and less than 10% impact on surge height. Only a thorough investigation of the behaviour of the coupled ocean-atmosphere system can shed more light on the importance of using the proper formulation of the drag coefficient.

Often models are run uncoupled. For instance, the wind from an atmosphere model is used to drive a wave model. In such a case it is very important to use the same drag formulation in both models to account for the coupled nature of the problem and avoid inconsistencies between the two models. This aspect has been stressed before by Van den Brink et al. (2013).

References

Bye, John A.T., and Jörg-Olaf Wolff (2004): Prediction of the drag law for air-sea momentum exchange. *Ocean Dyn.*, 54, 577580

Bryant, Kyra M., and Muhammad Akbar (2016): An exploration of wind stress calculation techniques in hurricane storm surge modeling. *J. Mar. Sci. Eng.*, 58, doi:10.3390/jmse4030058

Bye, John A.T., and Alastair D. Jenkins (2006): Drag coefficient reduction at very high wind speeds. *J. Geophys. Res.*, 111, C03024, doi: 10.1029/2005JC003114

H. Charnock (1955): Wind stress on a water surface. *Q. J. R. Meteorol. Soc.*, 81, 639-640

Donelan, M.A., B.K. Haus, N. Reul, W.J. Plant, M. Stiassnie, H.C. Graber, O.B. Brown, and E.S. Saltzman (2004): On the limiting aerodynamic roughness of the ocean in very strong winds. *Geophys. Res. Lett.*, 31, L18306, doi: 10.1029/2004GL019460

Druzhinin, O.A., Yu.I. Troitskaya, and S.C. Zilitienkevich (2017): The study of droplet-laden turbulent airflow over waved water surface by direct numerical simulation. *J. Geophys. Res. Oceans*, 122, 1789-1807, doi: 10.1002/2016JC012134

Emanuel, K.A. (1995): Sensitivity of tropical cyclones to surface exchange coefficients and a revised steady-state model incorporating eye dynamics. *J. Atmos. Sci.*, 52, 3969-3976

Fernandez, D.E., J.R. Carswell, S. Frasier, P.S. Chang, P.G. Black, and F.D. Marks (2006): Dual-polarized C- and Ku-band ocean backscatter response to hurricane-force winds. *J. Geophys. Res.*, 111, C08013, doi: 10.1029/2005JC003048

Hersbach, Hans, Ad Stoffelen, and Sybren de Haan (2007): An improved C-band scatterometer ocean geophysical model function: CMOD5. *J. Geophys. Res.*, 112, C03006, doi: 10.1029/2006JC003743

Hara, T., and S. E. Belcher (2002): Wind forcing in the equilibrium range of wind-wave spectra. *J. Fluid Mech.*, 470, 223-245

Hara, T., and S. E. Belcher (2004): Wind profile and drag coefficient over mature ocean surface wave spectra. *J. Phys. Oceanogr.*, 34, 2345-2358

Holland, G.J. (1980): An analytic model of the wind and pressure profiles in hurricanes. *Mon. Weather. Rev.*, 108, 12121218

Holthuijsen, Leo H., Mark D. Powell, and Julie D. Pietrzak (2012): Wind and waves in extreme hurricanes. *J. Geophys. Res.*, 117, C09003, doi: 10.1029/2012JC007983

Jarosz, E., D.A. Mitchell, D.W. Wang, and W.J. Teague (2007): Bottomup determination of air-sea momentum exchange under a major tropical cyclone. *Science*, 315, 1707-1709, doi: 10.1126/science.1136466. Supporting online material at `www.sciencemag.org/cgi/content/full/315/5819/1707/DC1`

Kudryavtsev, Vladimir N. (2006): On the effect of sea drops on the atmospheric boundary layer. *J. Geophys. Res.*, 111, C07020, doi: 10.1029/2005JC002970

Kudryavtsev, Vladimir N., and Vladimir K. Makin (2011): Impact of ocean spray on the dynamics of the marine atmospheric boundary layer. *Boundary-Layer Meteorol.*, 140, 383-410

Kudryavtsev, Vladimir N., Vladimir K. Makin, and S. Zilitinkevich (2012): On the sea-surface drag and heat/mass transfer at strong winds. Royal Netherlands Meteorological Institute (KNMI) WR2012(02), 28 pp., `http://bibliotheek.knmi.nl/knmipubWR/WR2012-02.pdf`

Large, W.G., and S. Pond (1981): Open ocean momentum flux measurements in moderate to strong winds. *J. Phys. Oceanogr.*, 11, 324-336

Makin, Vladimir K. (2005): A note on the drag of the sea surface at hurricane winds. *Boundary-Layer Meteorol.*, 115, 169-176, doi: 10.1007/s10546-004-3647-x

Miller, Banner I. (1968): A study of the filling of hurricane Donna (1960) over land. *Mon. Weath. Rev.*, 92, 389-406, doi: 10.1175/1520-0493(1964)092<0389:ASOTFO>2.3.CO;2

Moon, Il-Ju, Isaac Ginis, and Tetsu Hara (2004): Effect of surface waves on air-sea momentum exchange. Part II: Behavior of drag coefficient under tropical cyclones. *J. Atmos. Sci.*, 61, 2334-2348,

doi: 10.1175/1520-0469(2004)061<2334:EOSWOA>2.0.CO;2

Moon, Il-Ju, Isaac Gines, Tetsu Hara, and Biju Thomas (2007): A physics-based parameterization of air-sea momentum flux at high wind speeds and its impact on hurricane intensity predictions. *Mon. Weath. Rev.*, 135, 2869-2878, doi: 10.1175/MWR3432.1

Nicholls, S. (1985): Aircraft observations of the Ekman layer during the Joint Air-Sea Interaction Experiment. *Q. J. R. Meteorol. Soc.*, 111, 391-426

Ocampo-Torres, F.J., M.A. Donelan, N. Merzi, and F. Jia (1994): Laboratory measurements of mass transfer of carbon dioxide and water vapour for smooth and rough flow conditions. *Tellus*, B46, 16-32

Powell, Mark D., Peter J. Vickery, and Timothy A. Reinhold (2003): Reduced drag coefficient for high wind speeds in tropical cyclones. *Nature*, 422, 279-283, doi: 10.1038/nature01481

Portabella, M., and A. Stoffelen (2009): On scatterometer ocean stress. *J. Atmos. Ocean. Techn.*, 26, 368-382, doi: 10.1175/2008JTECHO578.1

Richter, David H., and Peter P. Sullivan (2013): Sea surface drag and the role of spray. *J. Geophys. Res.*, 40, 656-660, doi:10.1002/grl.50163

Smith, S.D., and E.G. Banke (1975) Variation of the sea surface drag coefficient with wind speed. *Q.J.R. Meteorol. Soc.*, 101, 665-673, doi: 10.1002/qj.49710142920

Tennekes, H. (1973): The logarithmic wind profile. *J. Atmos. Sci.*, 30, 234-238

Van den Brink, Henk, Peter Baas and Gerrit Burgers (2013): Towards an approved model set-up for HARMONIE. Contribution to WP 1 of the SBW-HB Wind modelling project. `http://projects.knmi.nl/publications/fulltexts/towards_an_approved_model_setup_for_harmonie_sbw_milestone1_final.pdf`

Vatvani, D., N.C. Zweers, M. van Ormondt, A.J. Smal, H. de Vries, and V.K. Makin (2012): Storm surge and wave simulations in the Gulf of Mexico using a consistent drag relation for atmospheric and storm surge models. *Nat. Hazards Earth Syst. Sci.*, 12, 2399-2410, `www.nat-hazards-earth-syst-sci.net/12/2399/2012`, doi: 10.5194/nhess-12-2399-2012

Walsh, Kevin J.E., P. Sandery, G.B. Brassington, M. Entel, C. SiegenthalerLeDrian, Jeffrey D. Kepert, and R. Darbyshire (2010): Constraints on drag and exchange coefficients at extreme wind speeds. *J. Geophy. Res.*, 115, C09007, doi:10.1029/2009jc005876

Wu, Jin (1982): Wind-stress coefficients over sea surface from breeze to hurricane. *J. Geophys. Res.*, C87, 9704-9706, doi: 10.1029/JC087iC12p09704

Yelland, M., and P.K. Taylor (1996): Wind measurements from the open ocean. *J. Phys. Oceanogr.*, 26, 541-558

Zweers, N.C., V.K. Makin, J.W. de Vries, and G. Burgers (2010): A sea drag relation for hurricane wind speeds. *Geophys. Res. Lett.*, 37, L21811, doi: 10.1029/2010GL045002

Zweers, N.C., V.K. Makin, J.W. de Vries, G. Burgers (2012): On the influence of changes in the drag relation on surface wind speeds and storm surge forecasts. *Nat. Hazards*, 62, 207-219, doi: 10.1007/s11069-011-9989-z

Zweers, N.C., V.K. Makin, J.W. de Vries, and V.N. Kudryavtsev (2015): The impact of spray-mediated enhanced enthalpy and reduced drag coefficients in the modelling of tropical cyclones. *Boundary-Layer Meteorol.*, 155, 501-514, doi: 10.1007/s10546-014-9996-1

Zijlema, M., G.Ph. van Vledder, and L.H. Holthuijsen (2012): Bottom friction and wind drag for wave models. *Coastal Engineering*, 65, 19-26, doi: 10.1016/j.coastaleng.2012.03.002